Progress In Electromagnetics Research C, Vol. 64, 117–123, 2016

Ultra-Thin 3D Printed All-Dielectric Antenna

Carlos Rodriguez, Jose Avila, and Raymond C. Rumpf*

Abstract—In this work we report an ultra-thin all-dielectric antenna that was designed, built, tested, and compared with simulated data. The objective of this research was to develop an antenna that is easily manufactured by common 3D printers available today. 3D printing is quickly revolutionizing manufacturing and the need to incorporate electrical elements like antennas is rising. Multi-material 3D printing that can build parts with conductors and dielectrics is the future, but at present it is very immature and largely inaccessible. The antenna presented here represents our first steps in developing all-dielectric antennas that can be manufactured today with commonly available 3D printers and materials. A monolithic antenna would have additional mechanical benefits when subjected to bending or thermal cycling. With this goal in mind, an ultra-thin all-dielectric antenna was developed. The antenna operates by taking advantage of total internal reflection and exciting a leaky whispering gallery mode. The antenna reported here operates at 2.4 GHz and was able to be as thin as 1.5 mm.

1. INTRODUCTION

Hybrid 3D printing (i.e., plastic + metal) is still in its infancy so producing electromagnetic elements like antennas remains challenging. References [1–3] introduce antennas that were manufactured by intricate 3D printing techniques. These antennas were designed in complex form factors and used conductive ink or spray, which is not typically available in low-cost 3D printers. The goal of the research presented here was to explore all-dielectric antennas that could be manufactured using standard fused deposition modeling (FDM) 3D printers. All-dielectric antennas have been demonstrated in [4, 5], but these antennas operate at optical frequencies which, when scaled to microwave frequencies, are no longer compact. To avoid costly and timely builds, it was desired to minimize the thickness as much as possible. A popular dielectric antenna is the dielectric resonator antenna (DRA), introduced as a radiating source in [6]. Much research has taken place with DRAs [7] and common methods to reduce the size is to introduce metal [8], or to increase the permittivity [9]. To date, the thinnest all-dielectric antenna reported in the literature is the dielectric resonator antenna (DRA) described in [10]. This antenna, however, incorporated a metal ground plane and the DRA required a relative permittivity of 1000 to be as thin as it was. We explored a different concept that avoided metal and significantly reduced the thickness of the antenna in order to achieve our goals. With such thin structures, traditional resonances were nearly impossible to achieve because the reflections at the edge of the antenna were extremely weak. To establish a resonance in a very thin slab of dielectric, the reflection at the edges was enhanced using a larger angle of incidence. A prism is effectively formed when a beam reflects off multiple interfaces within a structure at some larger angle of incidence. We call it a dielectric prism antenna (DPA) because it operates similar to an optical prism where light reflects from multiple surfaces through total internal reflection (TIR) as depicted in Figure 1(a).

Received 6 February 2016, Accepted 4 May 2016, Scheduled 26 May 2016
* Corresponding author: Raymond C. Rumpf (rcrumpf@utep.edu).
The authors are with the University of Texas at El Paso, El Paso, TX 79968, USA.

2. DESIGN AND MANUFACTURING

To develop the DPA efficiently, we studied it in stages of increasing numerical complexity. We first performed a one-dimensional simulation of an infinite dielectric slab waveguide using the finite-difference method in order to verify that a thin dielectric sheet is feasible for supporting an electromagnetic mode. For this simulation, the thickness of the slab was chosen to be 2.5 mm and the operating frequency was set to 2.4 GHz. The relative permittivity was chosen to be 20, as this is a reasonable value that could be realized in our lab. From the results of this analysis, it was found that two modes were supported by the slab. One mode is polarized horizontally within the plane of the slab while the other mode is polarized vertically out of the plane. The vertically polarized mode, however, was extremely large and extended outside of the slab by around $10\lambda_0$, where λ_0 is the free space wavelength, making it much more sensitive to its surrounding environment. Consequently, we concluded that exciting the horizontally polarized mode depicted in Figure 1(b) was favorable since it was so well confined to the slab making it less sensitive to its surrounding environment. It was found that the horizontally polarized mode had an effective refractive index of $n_{\text{eff}} = 1.6$. Symmetric dielectric slab waveguides have no cutoff frequency so, in principle, this antenna can be made even thinner.

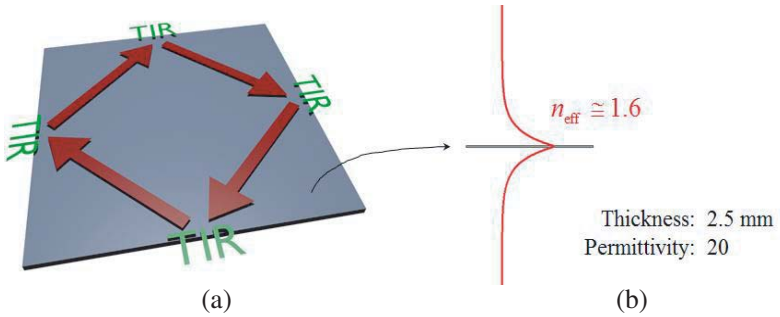

Figure 1. (a) Concept of a dielectric prism antenna. (b) Electromagnetic mode supported by a very thin slab of dielectric.

Our next step was to determine if this mode would resonate in a square shaped element. Reflections at the edges would be weak due to the low effective refractive index seen by the supported mode. We reasoned the reflections could be amplified by launching the mode at an angle above the critical angle, allowing us to pursue the concept of total internal reflection (TIR) as a means to establish resonance. It was possible to increase the angle of incidence even more by using a polygon with more sides. In the limit, this converges to a circular geometry as shown in Figure 2. For this reason, our DPAs were circular.

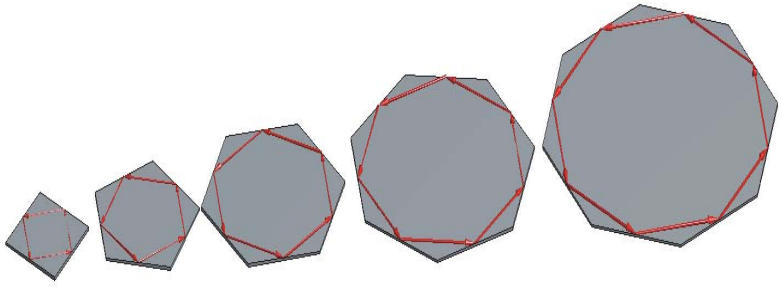

Figure 2. Convergence to a circular geometry.

The next step in our design process was to confirm that the DPA would support a circulating mode and radiate effectively. To do this in a fast and efficient manner, two-dimensional simulations were performed using the finite-difference frequency-domain (FDFD) method [11]. In these 2D simulations, the relative permittivity of the DPA was set to the effective permittivity calculated from the slab

waveguide simulations performed previously, $\varepsilon_{\text{eff}} = n_{\text{eff}}^2$. The permittivity outside of the DPA was set to air. The visualized fields from a FDFD simulation of a square DPA are shown in Figure 3(a) and of a circular DPA are shown in Figure 3(b). This shows the mechanism of resonance of the DPA and can be interpreted as leaky whispering gallery modes. In principle, it should be possible to reduce the thickness to any extent as along as the antenna area is made large enough so that reflections are sufficiently enhanced at the edges.

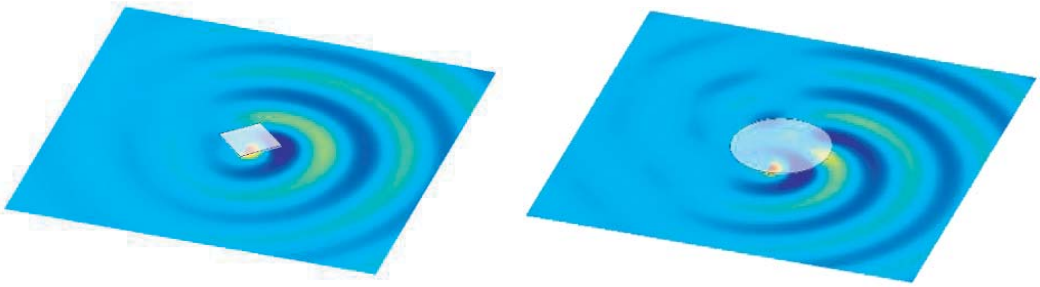

(a) (b)

Figure 3. (a) Resonance and radiation from a square DPA. (b) Resonance and radiation from a circular DPA.

Since no materials are currently commercially available for 3D printing with a relative permittivity of 20, we designed a thin plastic shell that we filled with dielectric powder supplied by Laird Technologies [12]. The diameter was 14.0 cm with a total height of 4.3 mm. The high permittivity region inside the shell which represents the actual antenna had a thickness of 2.8 mm and a diameter of 13.5 cm. To prevent bulging at the center of the DPA, a snap lid was designed that worked like a compact disk (CD) case as shown in Figure 4. The shell was manufactured from ordinary ABS plastic using a Makerbot Replicator 2X.

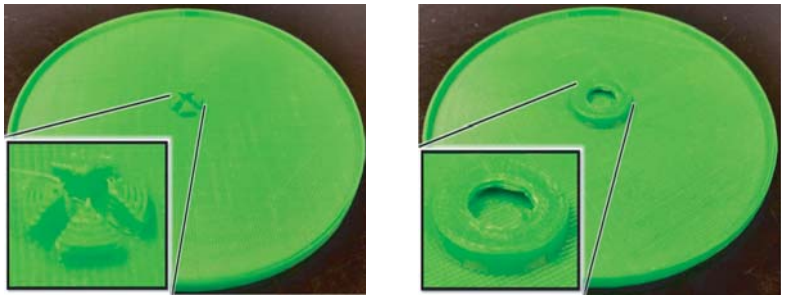

(a) (b)

Figure 4. (a) Top lid of the DPA shell. (b) Bottom lid of the DPA shell.

In order to excite this antenna with a horizontally polarized electromagnetic mode, a coaxial feed was made by separating the shielding from the center conductor along some length at the end of the cable to form a "V" shape. Figure 5(a) is a photograph of the entire coaxial cable modified into our feed, and Figure 5(b) shows a close-up of the feed taped on top of one of our 3D printed antennas. The outer shielding was soldered to improve performance.

3. SIMULATION RESULTS

Rigorous 3D simulations were performed using Ansys HFSS to fully evaluate the performance of the DPA, optimize the position of the feed, and generate a radiation pattern. The simulations showed that the excited mode couples into the DPA by simply placing the V on top of the antenna. Using the

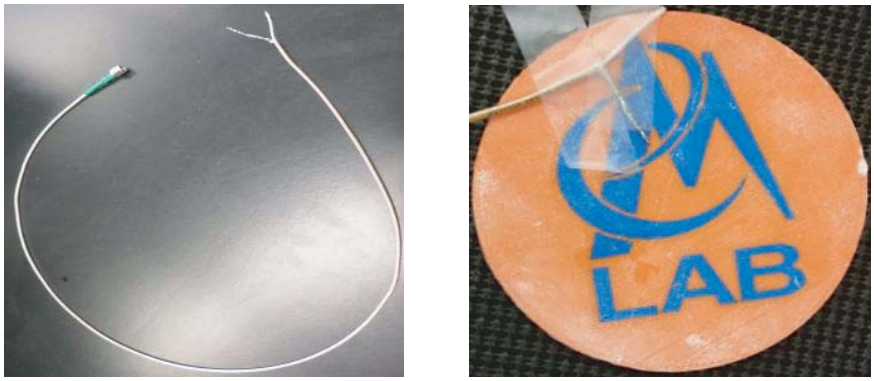

(a) (b)

Figure 5. (a) Structured feed from coaxial cable. (b) Close up of feed on a 3-D printed antenna.

parametric tool in HFSS, we discovered that certain optimized positions exist where the mode would circulate. An important attribute that these optimizations shared was that the tip of the probe needs to be positioned at the edge of the antenna for the mode to circulate. Figure 6(a) shows our simulation set up which superimposes the arrangement of all of the components involved so that it was as realistic and as closely matched to the experimental measurements as possible. Additionally, the figure shows that the radiation pattern consisted of multiple lobes. We were anticipating a smoother pattern shaped a bit like a conch shell. We determined that refraction caused our launched mode to bend slightly from the ideal circulating mode, causing discrete reflections with distinct peaks in the radiation pattern. A plot of the efficiency for our antenna with thickness of 1.5 mm and diameter of 13.5 cm is shown in Figure 6(b). At a resonance of 2.4 GHz, we can see that it reaches an efficiency of approximately 95%. We reason that the small amount of loss observed in the simulation was due primarily to the conductivity of the metals in the feed.

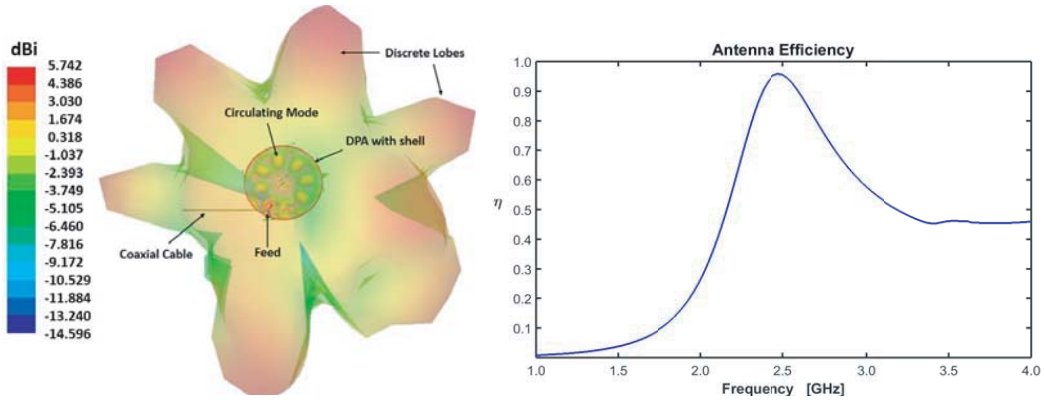

(a) (b)

Figure 6. (a) Detailed diagram of simulation with superimposed radiation pattern. (b) Radiation efficiency for the DPA of 1.5 mm thickness designed at 2.4 GHz.

Next, through simulation we studied the impact of the thickness of the slab and the radius of the circular DPA. The radiation pattern for our preliminary DPA having a thickness of 2.8 mm is shown in Figure 7(a). Figure 7(b) shows the radiation pattern for a DPA of a thickness of 1.5 mm. From the radiation patterns, it is concluded that the thinner the DPA is made, the weaker the resonance is because the circulating mode leaks more quickly. We can also see in Figure 8 that decreasing the radius produces fewer lobes. This second observation is due to the weaker resonance producing less circulation of the mode.

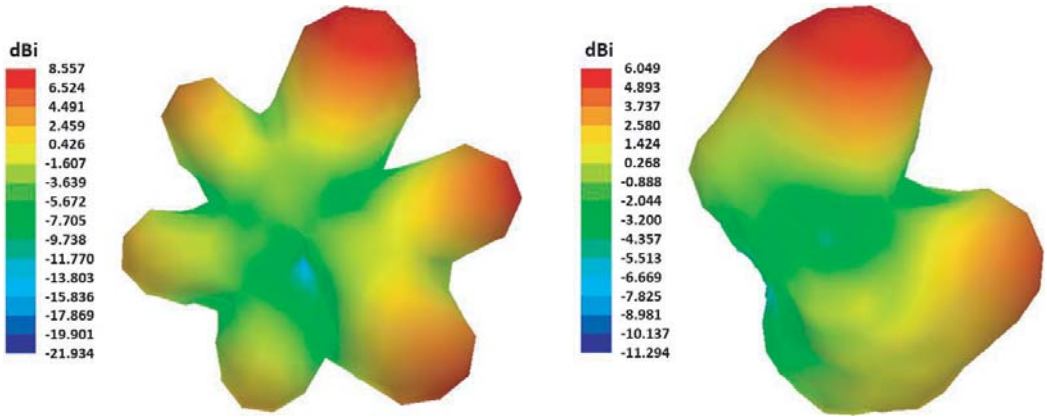

Figure 7. (a) Radiation pattern for DPAs of 2.8 mm thickness. (b) Same for 1.5 mm thickness.

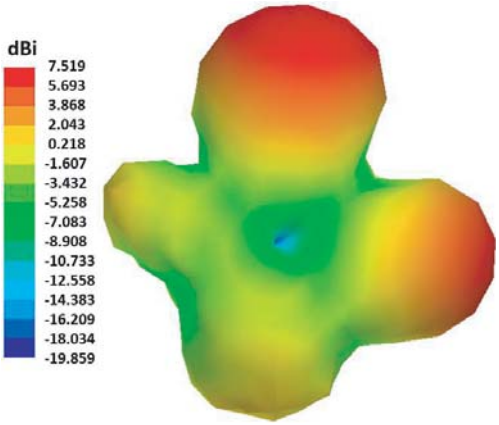

Figure 8. Radiation pattern for DPA with a diameter of 10.5 cm and a thickness of 2.8 mm.

4. EXPERIMENTAL RESULTS

An Agilent N5245 PNA-X vector network analyzer (VNA) was used to measure and experimentally optimize the response of the feed by trimming the pole lengths and determining the ideal feed placement. For a strong resonance at 2.4 GHz, we empirically found the best location of the feed to be around the bottom center extending towards the edge of the DPA. Figure 9 shows the optimized feed position and its dimensions for our 2.8 mm thick antenna. Two DPAs were manufactured and measured with our VNA in our anechoic chamber. Figure 10(a) shows the measured S_{11} for the DPA of thickness of 2.8 mm, with the superimposed simulated S_{11}. Figure 10(b) shows the same data for the DPA with thickness of 1.5 mm. Comparing these results we can see that they are closely matched and the antennas operate at the designed frequency of 2.4 GHz.

Radiation pattern results for our DPAs were measured in our anechoic chamber and are shown in the figures below. For our setup, we stationed a receiving horn antenna to capture the horizontal polarization at 0° while manually rotating the DPA in 10° increments. Some noise was introduced into our pattern measurements because it was difficult to keep the feed in a fixed and firm position while rotating the antenna. Figure 11 shows that the measured and simulated results agree and that the antenna is radiating with discrete lobes as opposed to a more uniform pattern. This is because as with the simulation the circulating mode is actually reflecting at discrete locations instead of circulating smoothly. The normalized radiation patterns also show that there is a direction in which a large amount of energy leaks in comparison. Future work will focus how to more effectively excite the circulating mode.

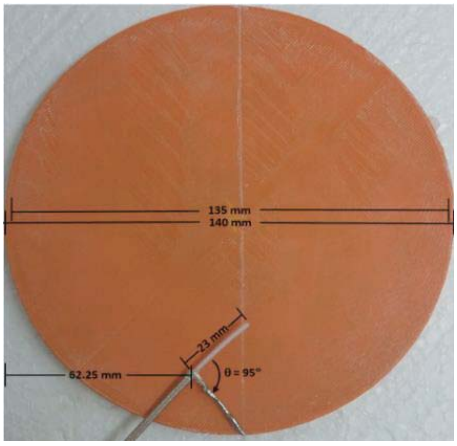

Figure 9. Optimized feed position for the DPA of 2.8 mm thickness designed at 2.4 GHz.

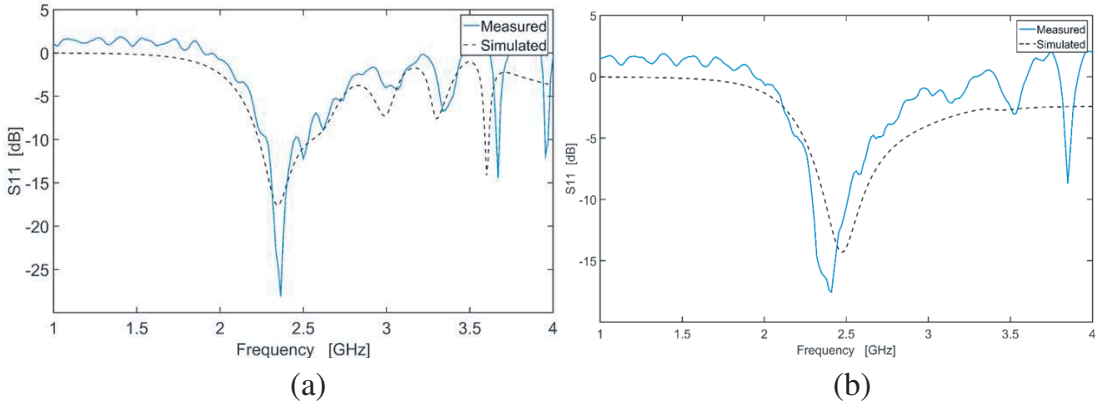

Figure 10. (a) Measured and simulated S_{11} for the DPA with thickness of 2.8 mm. (b) Measured and simulated S_{11} for the DPA with thickness of 1.5 mm.

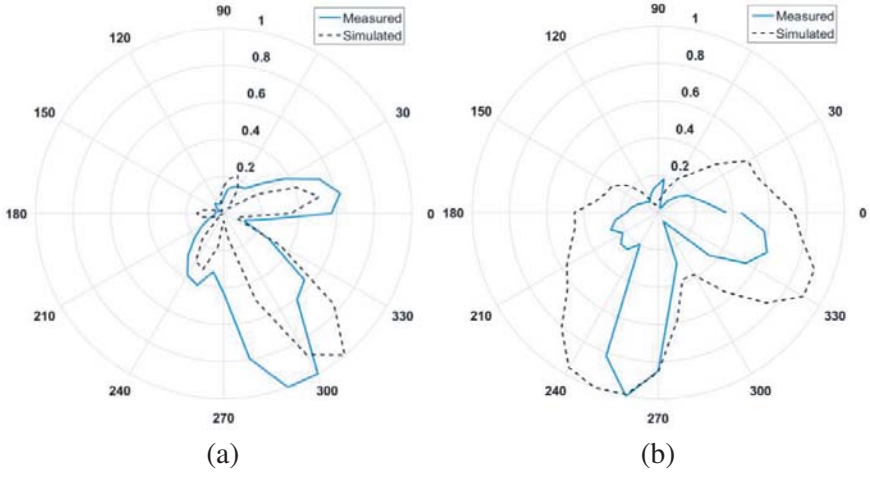

Figure 11. (a) Normalized radiation pattern for the 2.8 mm thick DPA. (b) Normalized radiation pattern for the 1.5 mm thick DPA.

5. CONCLUSION

In this paper an ultra-thin all-dielectric radiating structure was designed, 3D printed, simulated, and tested. Our antenna was designed to operate at 2.4 GHz, but it could be scaled to operate at virtually any frequency. The work described here produced the thinnest all-dielectric antenna yet reported in the literature. Its thin design and form factor make the antenna easy to manufacture using commonly available 3D printers. Future work in this area may concentrate on utilizing lower permittivity material to make realization even easier.

ACKNOWLEDGMENT

We thank Laird Technologies [12] for supplying the high-k powders used to build and test our antennas.

REFERENCES

1. Ahmadloo, M. and P. Mousavi, "Application of novel integrated dielectric and conductive ink 3D printing technique for fabrication of conical spiral antennas," *Antennas and Propagation Society International Symposium*, 780–781, July 2013.
2. Floch, J. M., B. Jaafari, and A. El Sayed Ahmed, "New compact broadband GSM/UMTS/LTE antenna realised by 3D printing," *2015 European Conference on Antennas and Propagation (EuCAP)*, 1–4, May 2015.
3. Andriambeloson, J. A. and P. G. Wiid, "Hyperband conical antenna design using 3D printing technique," *Radio and Antenna Days of the Indian Ocean*, 1–2, September 2015.
4. Krasnok, A. E., et al., "Ultracompact all-dielectric superdirective antennas," arXiv preprint arXiv:1211.0230, 2012.
5. Krasnok, A. E., et al., "All-dielectric optical nanoantennas," *Optics Express*, Vol. 20, No. 18, 20599–20604, 2012.
6. Long, S. A., M. W. McAllister, and L. C. Shen, "The resonant cylindrical dielectric cavity antenna," *IEEE Transactions on Antennas and Propagation*, Vol. 31, No. 3, 406–412, May 1983.
7. Petosa, A. and A. Ittipiboon, "Dielectric resonator antennas: A historical review and the current state of the art," *IEEE Antennas and Propagation Magazine*, Vol. 52, No. 5, 91–116, 2010.
8. Mongia, R. K., "Reduced size metallized dielectric resonator antennas," *IEEE International Symposium on Antennas and Propagation*, 2202–2205, Montreal, Canada, June 1997.
9. Mongia, R. K., A. Ittipiboon, and M. Cuhaci, "Low Profile dielectric resonator antennas using a very high permittivity material," *IEEE Electronics Letters*, Vol. 30, No. 17, 1362–1363, August 1994.
10. Ain, M. F., S. I. S. Hassan, M. Singh, M. A. Othman, B. M. Nawang, S. Sreekatan, S. D. Hutagalung, and Z. A. Ahmad, "2.5 GHz Batio3 dielectric resonator antenna," *Progress In Electromagnetics Research*, Vol. 76, 201–210, 2007.
11. Rumpf, R. C., "Simple implementation of arbitrarily shaped total-field/scattered-field regions in finite-difference frequency-domain," *Progress In Electromagnetics Research B*, Vol. 36, 221–248, 2012.
12. Laird Tech., "Hi-K Powder," 1825 Diamond Street, San Marcos, CA 92078, USA, Retrieved from http://www.lairdtech.com, March 19, 2015.